INT. J. NUM. METH. HEAT FLUID FLOW, VOL. 6, 77–90 (1996)

CONJUGATE HEAT TRANSFER ANALYSIS OF FLUID FLOW IN A PHASE-CHANGE ENERGY STORAGE UNIT

HONGJUN LI, C. K. HSIEH AND D. Y. GOSWAMI

Mechanical Engineering Department, University of Florida, Gainesville, FL 32611, USA

ABSTRACT

A method has been developed for conjugate heat transfer analysis of fluid flow inside parallel channels formed by a phase change material (PCM) separated from the fluid by a wall. The phase change in the PCM is two dimensional and a hybrid analysis consisting of an analytical solution in one direction and a finite-difference method in another direction is used to solve for the temperature in the PCM. The heat transfer fluid (HTF) inlet temperature is given and the heat transfer between the HTF and the PCM is treated as a conjugate problem that requires no iterations to obtain a solution. The numerical results are found to be stable, convergent, and accurate. Application of the method to the solution of heat extraction from a phase-change energy storage unit is given in detail and the numerical results are shown to be accurate, based on an energy conservation analysis, to within 3%.

KEY WORDS Conjugate heat transfer Phase change Finite difference

INTRODUCTION

Stefan problems that have been solved in the literature are mostly limited to phase change in a one-dimensional space. For these problems, solutions are mostly obtained for phase change with conditions fully specified at the boundary of the domain. This may not be applicable to a situation when the phase change material (PCM) is contained behind a wall and the phase change is caused by a fluid flowing over the other side of the wall. In this case, the condition at the boundary of the PCM is unknown *a priori*, while the fluid inlet temperature is given. The heat transfer in the PCM is two-dimensional. This problem is encountered in the design of energy storage systems. Yet, there has been a lack of studies dealing with the solution of this problem.

It has long been established that the two-dimensional Stefan problem described above cannot be solved exactly. An early approximate solution of the problem in a two-dimensional space was attempted by Poots[1] who extended the heat balance integral method of Karman and Pohlhausen[2] and reduced the mathematical problem of finding the two-dimensional solidification front into a numerical integration of a first-order ordinary differential equation. His numerical results have shown to be in good agreement with those found by Allen and Severn[3] who used a relaxation method. The two-dimensional Stefan problems can also be solved by using an embedding method, as shown by Sikarski and Boley[4]. In this method, the problem is reduced to a set of simultaneous integro-differential equations which can be solved either numerically or in a series form. Following a different approach, Rathjen and Jiji[5] combined Lightfoot's moving heat source method in one dimension[6] and Patel's treatment of the Stefan condition in multiple dimensions[7] for an analytical solution of the Stefan problem in a ninety-degree corner. Budhia and Kreith[8] followed a similar approach and solved the phase change in a planar wedge. In these studies, the interface position must be expressed in a functional form, with arbitrary constants, which are solved analytically. The success of the method thus hinges on the use of a proper function for the position.

0961–5539/96/030077–14$2.00

Received August 1994
Revised April 1995

Stefan problems in two dimensions can be solved numerically. Numerical methods using enthalpy formulation[9,10] yield satisfactory results when the phase change occurs over a small temperature range and the process occupies several nodal points of the spatial grid. This calls for the use of fine grids, which also restricts the maximum time-step size thus increasing the computing time. Meyer[11] and Shamsundar and Sparrow[12] used an implicit finite-difference method in conjunction with nodal iterations to solve such problems. Yao and Prusa[13] made a critical review of the enthalpy method in a monograph. Stafan problems can also be solved by a boundary fixing technique[14], which requires the iterative solution of complex equations. Sparrow *et al.*[15] were able to avoid iterations by using a variable grid spacing near the phase change interface. Stefan problems in multiple dimensions have also been solved by continuously tracking the moving interface[16–19]. This can be accomplished by an explicit scheme, which is, however, restricted by the space-time ratio. It also requires a good estimation for solution initiation. The interface can also be tracked by an implicit scheme, which can be applied without space-time limitations. However, it leads to a set of nonlinear equations, which must be solved iteratively for the temperature and interface position and is a tedious operation. In the numerical solutions reviewed above, the problems have been solved by using a finite difference method with conditions fully specified at the boundary of the domain. Finite element methods have also been developed for the solution of the Stefan problems[20,21]. Recently, these problems have been solved by a boundary element method, a numerical scheme requiring discretizing only the boundary. However, it is still a lengthy process to locate the interface position which is a key step in successfully obtaining a solution[22–24].

It is the purpose of this paper to present a conjugate heat transfer method that encompasses a hybrid scheme comprising an analytical solution of phase change in one direction and a finite difference analysis in another direction. The analytical solution will be developed on the basis of a source-and-sink method, which has been shown to be accurate in solving the Stefan problems in a series of previous papers; see, for example, References 25 through 29. In these studies, an incremental linearization scheme is used to search for the interface position in one dimension. Then, by using a finite difference method for temperature in another direction, the two-dimensional interface motion can be determined in a hybrid fashion without iteration. In the source-and-sink method, the phase change can be solved with a smaller number of equations. The phase change in the PCM can be coupled with the fluid flow in a conjugate heat transfer analysis. The numerical results obtained in this paper will be tested for accuracy using an energy conservation analysis.

PROBLEM DESCRIPTION

The system under investigation is depicted in *Figure 1*. An incompressible heat transfer fluid (HTF) of constant properties is flowing inside a channel formed by two parallel plane walls

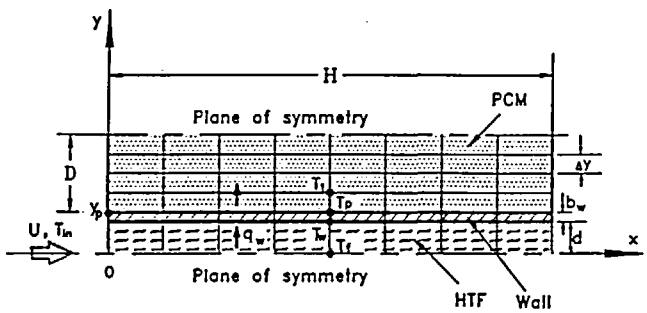

Figure 1 System for analysis

(only one half of the system is shown in the figure because of symmetry). Above the wall is the PCM which is insulated on the top and the left and the right boundaries, conditions suitable in the modeling of the heat transfer in energy storage systems. The HTF is well mixed in the y direction so that the heat transfer from the fluid to the wall can be analyzed by means of a convective heat transfer coefficient whose values can be obtained by using empirical equations. Heat transfer in the PCM is diffusion driven in a medium of equal and constant property values in different phase regions. The Peclet number of the HTF is large so that the heat conduction in the flow direction is negligibly small. Also, the channel wall is thin so that the heat conduction along the wall as well as the heat storage in the wall are both neglibible.

ANALYSIS

PCM

Diffusion of heat in the PCM in a two-dimensional space can be analyzed by using a source-and-sink method. In this method, a heat source is located at the freezing front while a heat sink is located at the melting front[25–27]. The governing equation takes the following form[25],

$$\nabla^2 T(\bar{r}, t)+\frac{L}{\alpha c} v_n(t)\delta(\bar{n}-\bar{n}_f)=\frac{1}{\alpha}\frac{\partial T(\bar{r}, t)}{\partial t}, \qquad \bar{r}\in(L\cup S),\ t>t_0 \tag{1}$$

where T is temperature, α is thermal diffusivity, v_n is the velocity of the interface motion in normal direction, t is time, and δ is a Dirac delta function in which $\bar{n}$ and $\bar{n}_f$ are the position vectors to a point and the interface position, respectively. Other notations have been defined in *Table 1*.

The initial and the boundary conditions are, respectively,

$$T(\bar{r}, t_0)=T_i(\bar{r}) \tag{2}$$

$$k_i\frac{\partial T}{\partial n_i}+h_i(T-T_\infty)=0, \qquad \bar{r}=\bar{r}_i, \quad i=1, 2, 3, 4 \tag{3}$$

Table 1 Input data for conjugate heat transfer analysis

PCM—$Na_3PO_4\cdot 12H_2O$	
Conductivity, k (W/m·K)	0.6
Heat capacity, c (kJ/kg·K)	1.7
Density, ρ (kg/m^3)	1630
Latent heat, L (kJ/m^3)	110
Melting point, T_m (°C)	72
HTF—Water	
Conductivity, k_f (W/m·K)	0.58
Heat capacity, c_f (kJ/kg·K)	4.19
Density, ρ_f (kg/m^3)	1000
Initial temperature, T_0 (°C)	80
HTF inlet temperature, $T_f(0, t)$ (°C)	23
Volume flow rate, $\dot{Q}$ (l/min (lpm))	3.78
	7.57
	11.35
Other specifications—	
PCM length, H (m)	2
PCM width, W (m)	0.5
PCM half thickness, D (m)	0.02
Channel width, $2d$ (m)	0.01
Number of PCM plates, M	4
Container wall thickness, b_w (m)	0.0

and the interface temperature condition is,

$$T(\bar{r}_f, t) = T_m \tag{4}$$

Here, the boundary condition (3) is taken to be a Robin condition so that setting k_i to zero reduces it to a Dirichlet condition. On the other hand, setting h_i (convective coefficient) to zero reduces it to a Neumann condition. Also for the sake of generality, the PCM is taken to be either subcooled or superheated initially. Equation (2) thus represents the initial temperature distribution in the PCM at t_0, when the phase change takes place. It is noted that (1) embodies the Stefan flux condition. This can be easily verified by integrating this equation across the phase change interface[25–28]. In the source-and-sink method, equations (1) through (4) are solved for temperatures in *all* phase regions, whereas in the conventional Neumann approach, one set of equations must be solved for the temperature in *each* phase region. These temperatures in different phase regions must be introduced into (4) and a *separate* Stefan condition to evaluate the interface motion, a lengthy operation for the Neumann approach.

For phase change in a two-dimensional space, the Dirac delta term in (1) can be expressed by using vector analysis as[30],

$$\frac{L}{\alpha c} v_n(t)\delta(\bar{n}-\bar{n}_f) = \frac{L}{\alpha c}\frac{\partial S}{\partial t}\delta[y - S(x, t)] \tag{5}$$

where $S(x, t)$ represents the interface position in the y direction. Substituting (5) into (1) gives the governing equation for phase change in two dimensions as,

$$\nabla^2 T(\bar{r}, t) + \frac{L}{\alpha c}\frac{\partial S}{\partial t}\delta[y - S(x, t)] = \frac{1}{\alpha}\frac{\partial T(\bar{r}, t)}{\partial t}, \qquad \bar{r} \in (L \cup S), \quad t > t_0 \tag{6}$$

Equation (6) can be solved by using a superposition as[30],

$$T(\bar{r}, t) = U(\bar{r}, t) + V(\bar{r}, t) \tag{7}$$

The subproblem $U(\bar{r}, t)$ can then be formulated as follows,

Governing Equation

$$\nabla^2 U(\bar{r}, t) = \frac{1}{\alpha}\frac{\partial U(\bar{r}, t)}{\partial t} \tag{8}$$

Initial Condition

$$U(\bar{r}, t_0) = T_i(\bar{r}) \tag{9}$$

Boundary Conditions

$$k_i \frac{\partial U}{\partial n_i} + h_i(U - T_\infty) = 0, \qquad \bar{r} = \bar{r}_i, \quad i = 1, 2, 3, 4 \tag{10}$$

The subproblem $V(\bar{r}, t)$ can be formulated as follows,

Governing Equation

$$\nabla^2 V(\bar{r}, t) + \frac{L}{\alpha c}\frac{\partial S}{\partial t}\delta[y - S(x, t)] = \frac{1}{\alpha}\frac{\partial V(\bar{r}, t)}{\partial t}, \qquad \bar{r} \in (L \cup S), \quad t > t_0 \tag{11}$$

Initial Condition

$$V(\bar{r}, t_0) = 0 \tag{12}$$

Boundary Conditions

$$k_i \frac{\partial V}{\partial n_i} + h_i V = 0, \qquad \bar{r} = \bar{r}_i, \qquad i = 1, 2, 3, 4 \tag{13}$$

For the numerical solution of the heat transfer in the PCM, the $U(\bar{r}, t)$ problem can be solved by an alternating-direction-implicit (ADI) method as will be shown later. As for the V problem, since the phase change is expected to be gradual in the x direction, the second partial of V with x can be changed to a finite difference form. Further, by indexing x with subscript i so that $V(x, y, t)$ is changed to $V_i(y, t)$ and $V(x\pm\Delta x, y, t)$ to $V_{i\pm1}(y, t)$, (11) can be re-cast as,

$$\frac{\partial^2 V_i(y,t)}{\partial y^2}+\frac{V_{i+1}(y,t)-2V_i(y,t)+V_{i-1}(y,t)}{\Delta x^2}+\frac{L}{\alpha c}\frac{\partial S_i}{\partial t}\delta[y-S_i(t)]=\frac{1}{\alpha}\frac{\partial V_i(y,t)}{\partial t},$$

$$\bar{r}\in(L\cup S), \qquad t>t_0 \quad (14)$$

Here, the temperature in the x and y directions has been decoupled to the extent that (14) represents a piecewise, axially related phase change problem in the y direction. Green's function can then be used to solve this equation. In this effort, the second and the third terms on the left hand side are collectively taken to be the heat generation terms, and this equation can be solved with a time-marching scheme. In this scheme, V_i at the end of the first time step at t_1, which is equal to t_0 plus Δt, can be derived as,

$$V_i(y,t_1)=\frac{L}{c}\int_{\tau=t_0}^{t_1}\frac{\partial S_i}{\partial\tau}G_i(y,t_1\,|\,S_i,\tau)\,d\tau+\alpha\int_{\tau=t_0}^{t_1}d\tau\int_{y'=0}^{D}g_i(y',\tau)G_i(y,t_1\,|\,y',\tau)\,dy' \quad (15)$$

Here, terms for the initial and boundary conditions have vanished because of the homogeneous conditions (12) and (13). In (15), $g_i(y', \tau)$ refers to,

$$g_i(y',\tau)=\frac{V_{i+1}(y',\tau)-2V_i(y',\tau)+V_{i-1}(y',\tau)}{\Delta x^2} \quad (16)$$

and $G_i(y, t_1\,|\,y', \tau)$ denotes the Green's function,

$$G_i(y,t_1\,|\,y',\tau)=\frac{2}{D}\sum_{m=1}^{\infty}\exp[-\alpha\beta_m^2(t_1-\tau)]\sin(\beta_m y)\sin(\beta_m y') \quad (17)$$

where $\beta_m=(2m-1)\pi/(2D)$, and $m=1, 2, \ldots$.

It is still not possible to solve (15) because the g function contains $V_{i\pm1}$ terms. One way to resolve this is to expand the g as,

$$g_i(y,t)=g_i(y,t_0)+\frac{\partial g_i(y,t_0)}{\partial t}(t-t_0) \quad (18)$$

It can be shown by using (12) and (16) that the first term on the right of (18) vanishes. As for the second term in this equation, it can be shown by using (16) that,

$$\frac{\partial g_i(y,t_0)}{\partial t}=\frac{1}{\Delta x^2}\left[\frac{\partial V_{i-1}(y,t_0)}{\partial t}-2\frac{\partial V_i(y,t_0)}{\partial t}+\frac{\partial V_{i+1}(y,t_0)}{\partial t}\right] \quad (19)$$

Further introduction of (11) and (12) permits V in (15) to be expressed as,

$$V_i(y,t_1)=\frac{L}{c}\int_{\tau=t_0}^{t_1}\frac{\partial S_i}{\partial\tau}G_i(y,t_1\,|\,S_i,\tau)\,d\tau+\frac{\alpha L}{c\,\Delta x^2}(w_{i+1}-2w_i+w_{i-1}) \quad (20)$$

where

$$w_j=\int_{\tau=t_0}^{t_1}(\tau-t_0)\frac{\partial S_j}{\partial\tau}G_i(y,t_1\,|\,S_j,\tau)\,d\tau, \qquad j=i+1,\ i,\ i-1 \quad (21)$$

HTF

Under the conditions given, the heat transfer in the fluid can be analyzed by using the following equation,

$$\frac{\partial T_f}{\partial t}+U\frac{\partial T_f}{\partial x}+\frac{h(T_f-T_w)}{\rho_f c_f d}=0 \tag{22}$$

with the inlet condition,

$$T_f(0,t)=T_{in}(t) \tag{23}$$

Notations used in these equations have been defined in *Table 1* and in the system diagram shown in *Figure 1*.

In the conjugate heat transfer analysis, heat convection from the fluid to the wall can be equated to the heat conduction into the PCM through its lower boundary. Thus,

$$h(T_f-T_w)=-k\frac{\partial T}{\partial y}\bigg|_{y=y_p} \tag{24}$$

At the lower boundary of the PCM, the temperature is related to the wall temperature as,

$$T_p=T_w-b_w q_w/k_w \tag{25}$$

In the numerical computation, the convective heat transfer coefficient is taken from the empirical equation[31],

$$Nu_D=\frac{(f/8)(Re_D-1000)Pr}{1+12.7(f/8)^{1/2}(Pr^{2/3}-1)} \tag{26}$$

where f is the friction factor. It is related to the Reynolds number as,

$$f=[0.79\ln(Re_D)-1.64]^{-2} \tag{27}$$

In these equations, the Nusselt and the Reynolds numbers are defined on the basis of the hydraulic diameter, D_h, as,

$$Nu_D=\frac{hD_h}{k_f},\qquad Re_D=\frac{UD_h}{v} \tag{28}$$

Equation (26) is valid for the Prandtl number in the range of 0.5 to 2000 and the Reynolds number in the range of 2300 to 5×10^6. The original equation was correlated on the basis of flow inside circular pipes; it has been adapted here for use in the straight channels by means of the hydraulic diameter as suggested in Reference 32.

Energy analysis

In the absence of data in the literature for comparison, the numerical results obtained in this paper are checked for accuracy by means of an energy conservation analysis. Following the first law of thermodynamics,

$$\begin{aligned}\int_{\tau=0}^{t}\dot{Q}\rho_f c_f[T_f(0,\tau)-T_f(H,\tau)]\,d\tau=2W\Bigg\{&\int_{y=0}^{D}dy\int_{x=0}^{H}\rho c[T(x,y,t)-T_0]\,dx\\&+\int_{x=0}^{H}[-L\rho S(x,t)]\,dx\\&+\int_{x=0}^{H}\rho_w c_w b_w[T_w(x,t)-T_0]\,dx\\&+\int_{x=0}^{H}\rho_f c_f d[T_f(x,t)-T_0]\,dx\Bigg\}\end{aligned} \tag{29}$$

This equation is written on the basis of energy being extracted from the PCM. The entire system is at a uniform temperature T_0 initially (superheated medium). The channel has a width W and the PCM has a thickness $2D$. In (29), the left hand side represents the energy gained by the HTF as it flows inside the channel. This energy comes from the sensible and latent heat changes of the PCM, the sensible heat change of the channel wall, and the temperature change of the HTF inside the channel (four terms on the right of the equation, respectively). Clearly, an accurate solution of the problem requires that the numerical values evaluated on both sides of the equation be equal. Any disagreement between the two serves as a measure of the inaccuracy in the solution.

NUMERICAL IMPLEMENTATION

The U problem can be solved by using an alternating-direction-implicit (ADI) method in a time-marching scheme as,

$$-\theta_x U^{n+1/2}_{i-1,j}+(1+2\theta_x)U^{n+1/2}_{i,j}-\theta_x U^{n+1/2}_{i+1,j}=\theta_y U^{n}_{i,j-1}+(1-2\theta_y)U^{n}_{i,j}+\theta_y U^{n}_{i,j+1} \tag{30}$$

$$-\theta_y U^{n+1}_{i,j-1}+(1+2\theta_y)U^{n+1}_{i,j}-\theta_y U^{n+1}_{i,j+1}=\theta_x U^{n+1/2}_{i-1,j}+(1-2\theta_x)U^{n+1/2}_{i,j}+\theta_x U^{n+1/2}_{i+1,j} \tag{31}$$

where

$$\theta_x=\frac{\alpha\Delta t}{2\Delta x^2}, \qquad \theta_y=\frac{\alpha\Delta t}{2\Delta y^2} \tag{32}$$

and i and j refer to indices in x and y directions, respectively. Equations (30) and (31) can be used to solve for the temperature even in the pre-melting and pre-solidification stages for a subcooled and superheated PCM, respectively.

Once phase change takes place at the boundary of the PCM, the V problem is engaged. In this problem, the interface position in the y direction is solved by using a linear approximation as[28,29],

$$S_i(t)=S_i(t_{n-1})+\frac{\partial S_i(t_{n-1})}{\partial t}(t-t_{n-1}) \tag{33}$$

Then the temperature V can be found at the end of each time step Δt. This temperature is then added to U to find T, which is, in turn, used as the condition for the temperature at the initiation of the succeeding time step. In the present work, the temperatures are superimposed at the end of each time step. Since only the U problem accounts for a non-zero initial condition, (20) can be used for all time steps. In this effort, the equation for $V_i(y, t_n)$ can be formulated by changing t_0 to t_{n-1} and t_1 to t_n in (20). A similar change will be made in (17) and (21).

In the solution of the Stefan problems for each time step, the interface position can be found by setting y to $S_i(t)$ and $V_i(y, t)$ to $T_m-U^n_{i,j}$ in (20). This equation is then solved implicitly for the interface position. Usually, the interface position may not fall exactly on the grid point j in the U problem. Then, a cubic spline will be used for interpolation in the y direction.

In the solution of the conjugate heat transfer problem consisting of both HTF and PCM, equation (24) can be used for matching. However, there are several unknowns in this equation and they cannot be found by using iteration because of stability concerns as reported by Barozzi and Pagliarini[33]. Moreover, the numerical results of iteration may not converge unless the initial guesses are good.

To alleviate these problems, the third term on the left of (22) is rewritten in terms of T_1, the temperature at the first interior grid point inside the PCM (see *Figure 1*). Thus,

$$h(T_f-T_w)=\frac{T_f-T_1}{R_t} \tag{34}$$

where R_t refers to the overall thermal resistance from the HFT to the PCM

$$R_t=\frac{1}{h}+\frac{b_w}{k_w}+\frac{\Delta y}{k_p} \tag{35}$$

In practice, if the interface position S is found to be less than the grid size Δy, T_1 in (34) is changed to T_m, the phase change temperature, and the Δy is changed to S.

The governing equation for the HTF can then be changed to,

$$\frac{\partial T_f}{\partial t}+U\frac{\partial T_f}{\partial x}+\frac{T_f-T_1}{\rho_f c_f R_t d}=0 \tag{36}$$

This equation can be solved by using a first-order accurate implicit finite difference scheme as,

$$T_{f,j}^{n+1}=\frac{T_{f,j}^{n}+\theta_1 T_{f,j-1}^{n+1}+\theta_2 T_1}{1+\theta_1+\theta_2} \tag{37}$$

where

$$\theta_1=\frac{U\,\Delta t}{\Delta x}, \qquad \theta_2=\frac{\Delta t}{\rho_f c_f R_t d} \tag{38}$$

The temperature imposed at the boundary of the PCM follows as,

$$T_p=\frac{R_1 T_1+R_2 T_f}{R_1+R_2} \tag{39}$$

where

$$R_1=\frac{1}{h}+\frac{b_w}{k_w}, \qquad R_2=\frac{\Delta y}{k_p} \tag{40}$$

The surface temperature given by (39) will then be used as the boundary condition for the solution of the phase change in the PCM.

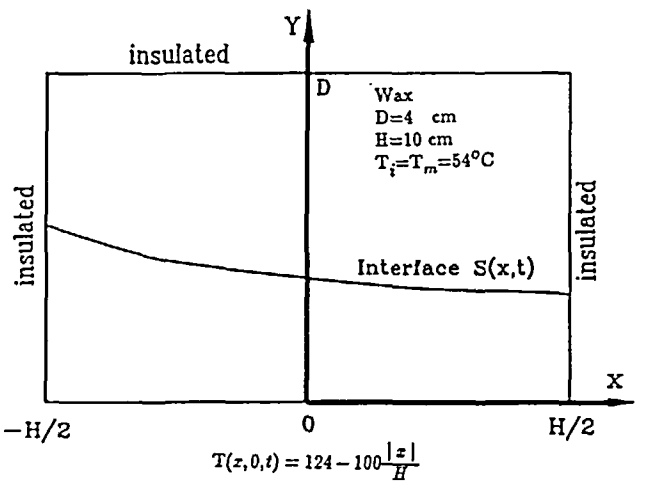

Figure 2 Problem used for two-dimensional stability and convergence tests

TESTS FOR STABILITY, CONVERGENCE, AND ACCURACY

Tests for stability, convergence, and accuracy proceed along two different lines. First, the numerical method for the solution of two-dimensional phase change in the PCM is tested for stability and convergence by solving a problem in a two-dimensional domain shown in *Figure 2*. In this problem, the bottom boundary is imposed with a space-variant temperature condition, while the other boundaries are all insulated. The PCM (wax) is initially in a solid state at its phase change temperature (54°C). It is thus a one-phase melting problem as soon as the temperature condition is imposed on the lower boundary.

To test the stability of the solution of this problem, a 40×30 grid is used in the x and y directions. The time step varies from 30 to 600 s, which corresponds to a dimensionless time-step size (Fourier modulus) of 0.5 and 10, respectively. *Figure 3* gives the history of the interface position at $x=0$ and $x=H/2$. Two groups of curves are plotted. In each group, the solid line is used to represent the analytical solution of a Stefan-Neumann problem imposed with a uniform temperature condition. The imposed temperature value corresponds to that calculated using the equation given in *Figure 2* at the specified point. Hence, the solid curves in *Figure 3* provide the upper bound for the interface position at x equal to zero and the lower bound for the position at x equal to $H/2$. The dashed curves give the numerical results for the solution of the two dimensional problem; they stay within bounds. Most importantly, all dashed curves are smooth and results converge nicely irrespective of the time-step size used.

Figure 4 gives the interface position in the two-dimensional domain at 3000 s. Four time-step sizes are tested. Again, the interface position curves are smooth and the results are convergent. No instability is encountered even with a time-step as large as 600 s. The explicit treatment of the partial differential in x by a finite difference in (14) thus introduces no instability in the solution of the V problem. It also points to the fact that, in the solution of the two-dimensional Stefan problem as given in this paper, the time-step sizes are determined strictly on the basis of accuracy rather than the stability. Better yet, the stability of the numerical solution is insensitive to the number of the grid points used in the x direction. For example, a reduction of the number of the grids in x by a factor of four (10×30 grid) together with the use of a time-step size of 300 s yields results (circles) which still fall on the curves. This also demonstrates the efficiency of the method.

The accuracy of the numerical solution has been tested rigorously as described in Reference 34. Briefly, the two-dimensional solution method described in this paper has been used to predict

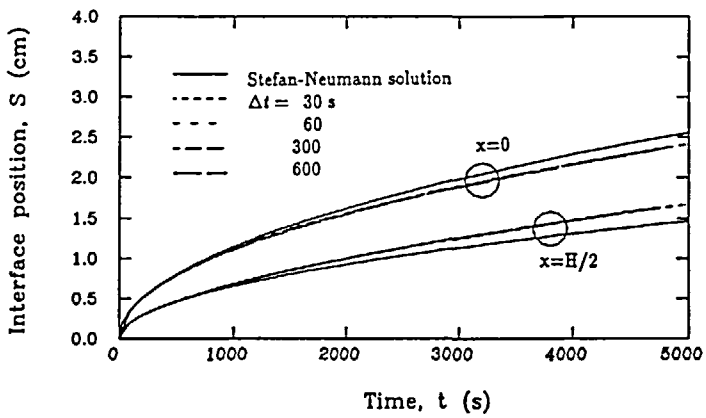

Figure 3 Interface-position history curves at $x=0$ and $x=H/2$

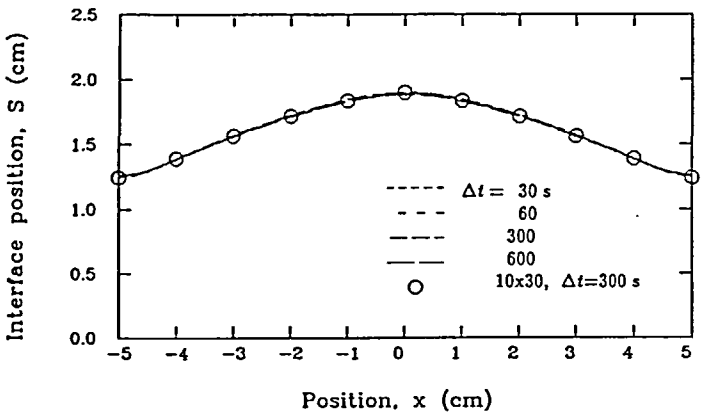

Figure 4 Interface-position curves at 3000 s tested for four time-step sizes

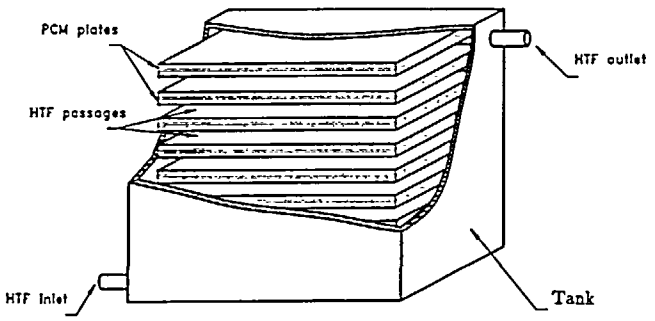

Figure 5 A schematic drawing for the analysis of a thermal-energy storage unit

the square-root time relationship for a one-dimensional phase change in a semi-infinite medium imposed with a constant temperature boundary condition. The present method has also been used to predict the steady state limit of the two-dimensional phase change interface position in a domain subjected to lateral heat loss from the boundary. This serves as a test on the accuracy of the method over a long period of time. Finally, an experiment measuring the position of the interface position in melting wax has also been performed for testing the accuracy of the solution over a short time. In all these tests, the numerical results have found to be accurate. Tests for the solution of the two-dimensional phase change in the PCM are now complete; its application to the development of conjugate heat transfer analysis consisting of both PCM and HTF will be tested in the section that follows.

RESULTS AND DISCUSSION

The conjugate solution method described in this paper is used to solve the heat transfer in a thermal-energy storage unit sketched in *Figure 5*. Here, the PCM is placed inside flat, plane-parallel containers spaced vertically apart so that the HTF is allowed to pass through the channels formed by the gap between these containers. Baffles are placed inside the tank so that the HTF flows evenly through all channels. Heat transfer in each channel can thus be analyzed by using the system diagram shown in *Figure 1*. *Table 1* provides a summary of the data used for input in the analysis. The initial temperature of the entire system is taken to be uniform at

80°C, while the PCM has a melting temperature of 72°C. The PCM is thus superheated in a decomposed state initially. Heat is extracted by passing cold water (HTF) through the system at three different flow rates. The total amount of heat stored initially in the system excluding the tank wall is calculated to be 63.5 MJ. In the numerical computation, calculation ceases once the water exit temperature drops down to 40°C, a threshold commonly used in the design of household water heaters.

As has been mentioned earlier, the conjugate solution results are to be tested for accuracy by using the energy analysis formulated in equation (29). *Figure 6* gives such a test. In this figure, the solid lines represent the energy change verus time for the left hand side of the equation, while the dashed lines represent that for the right hand side of the equation. At all flow rates, the maximum error is found to be close to 3% at the end of the energy discharging process. The method has thus shown to be accurate for engineering applications. In this test, a 41×21 grid is used in the PCM and a time step of 120 s is used in the computation. No instability was encountered.

The water exit temperatures during the heat extraction process are also plotted as shown in *Figure 7*. As expected, a smaller flow rate permits a longer time for the water to extract heat from the unit. At all flow rates, the water exit temperature appears to be somewhat erratic with time, which is believed to be a result of the phase change in the unit. In fact, the smoothness of the curves has much to do with the specific kind of heat, sensible or latent, that is released. In the case of the latent heat release, the water exit temperature also varies with the position of the interface that releases the latent heat. A deeper interface position tends to smooth the temperature curves as is evident from the curves plotted. The irregular temperature curves have also been found experimentally as reported by Saitoh and Hirose[35].

The temperature distribution in the PCM at 7.57 lpm flow rate is shown in *Figure 8*. Here, the plots are scaled in width and height for ease of viewing the isotherms. The topmost figure

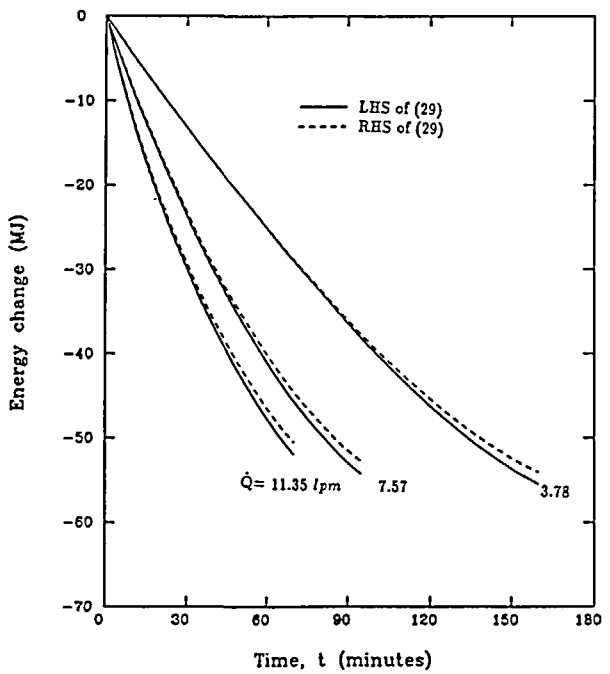

Figure 6 Test of accuracy by means of energy conservation

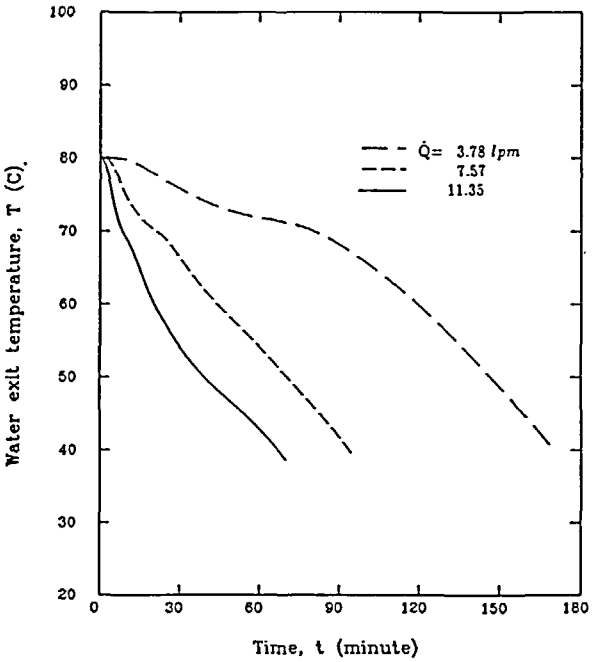

Figure 7 Water exit temperature versus time at different flow rates

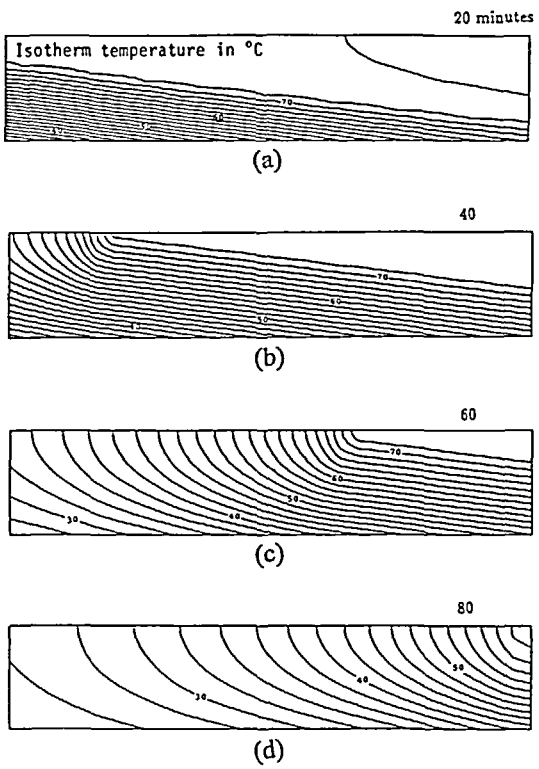

Figure 8 Isotherms in a half slab of the PCM

(a) gives the isotherm position in the PCM at 20 minutes. At this time, the lower part of the PCM has changed phase as shown by the high density of the isotherms in this region. Physically, there is a large temperature gradient there caused by the small thermal conductivity of the PCM. In this diagram, the interface position can be located by searching for the isotherm where its density changes abruptly. The PCM is still in the decomposed state in the upper right half of the domain. As time moves along to 40 minutes (*Figure* (b)), the left part of the PCM has changed phase completely while the decomposed region also diminishes in size. The PCM is totally changed phase over its entire region at 80 minutes (*Figure* (d)). At that time, the isotherms spread out evenly. In all plots in this figure, all isotherms are perpendicular to the top and the right boundaries of the PCM. They are not so, however, at the left boundary, which can be ascribed to the water inlet temperature and scaling of the plots as mentioned at the beginning of this paragraph.

CONCLUDING REMARKS

It is reiterated that, in *Figure 6*, the error is computed on the basis of an energy analysis. The error plotted thus represents a cumulative effect encompassing errors in the temperatures in the PCM and HTF as well as the interface position error in the PCM. Being less than 3% at the end of the heat extraction process at a time as long as 160 minutes provides confidence of the overall accuracy of the method. The hybrid-conjugate heat transfer analysis developed in this paper is thus useful in solving the energy storage problems.

REFERENCES

1 Poots, G. An approximate treatment of heat conduction problem involving a two-dimensional solidification front, *Int. J. Heat Mass Transfer*, **5**, 339–348 (1962)
2 Pohlhausen, K. Zur naherungsweisen integration der differentialgleichung der laminaren grenzschict, *ZAMM*, **1**, 252–268 (1921)
3 Allen, D. N. de G. and Severn, R. T. The application of relaxation methods to the solution of non-elliptic partial differential equations; III. Heat conduction, with change of state, in two dimensions, *Quart J. Mech. Appl. Math.*, **15**, 52–62 (1962)
4 Sikarski, D. L. and Boley, B. A. The solution of a class of two-dimensional melting and solidification problems, *Int. J. Solid Struct.*, **1**, 207–234 (1965)
5 Rathjen, K. A. and Jiji, L. M. Heat conduction with melting or freezing in a corner, *J. Heat Transfer*, **93**, 101–109 (1971)
6 Lightfoot, N. M. H. The solidification of molten steel, *Proc. Lond. Math. Soc.*, **31**, 97–116 (1929)
7 Patel, P. D. Interface condition in heat conduction problems with change of phase, *AIAA J.*, **6**, 2454–2456 (1968)
8 Budhia, H. and Kreith, F. Heat transfer with melting and freezing in a wedge, *Int. J. Heat Mass Transfer*, **16**, 195–211 (1973)
9 Elliot, C. M. and Ockendon, J. R. *Weak and Variational Methods for Moving Boundary Problems*, Pitman, London (1982)
10 Alexiades, V. and Solomon, A. D. *Mathematical Modeling of Melting and Freezing Processes*, Hemisphere, Washington (1993)
11 Meyer, G. H. Multidimensional Stefan problems, *SIAM J. Num. Anal.*, **10**, 522–538 (1973)
12 Shamsundar, N. and Sparrow, E. M. Analysis of multidimensional conduction phase change via the enthalpy model, *J. Heat Transfer*, **97**, 333–340 (1975)
13 Yao, L. S. and Prusa, J. Melting and freezing, *Adv. Heat Transfer*, **19**, 1–95 (1989)
14 Spaid, F. W., Chawart, A. F., Radekopp, L. G. and Rosen, R. Shape evolution of a subliming surface subjected to unsteady spatially nonuniform heat flux, *Int. J. Heat Mass Transfer*, **14**, 673–687 (1971)
15 Sparrow, E. M., Ramadhyani, S. and Patankar, S. V. Effect of subcooling on cylindrical melting, *J. Heat Transfer*, **100**, 395–402 (1978)
16 Murray, W. D. and Landis, F. Numerical and machine solutions of transient heat-conduction problems involving melting or freezing, *J. Heat Transfer*, **81**, 106–112 (1959)
17 Tien, L. C. and Churchill, S. W. Freezing front motion and heat transfer outside an infinite, isothermal cylinder, *AIChE J.*, **11**, 790–793 (1965)
18 Lazaridis, A. A numerical solution of the multidimensional solidification (or melting) problem, *Int. J. Heat Mass Transfer*, **13**, 1459–1477 (1970)
19 Meyer, G. H. Direct and iterative one-dimensional front tracking methods for the two-dimensional Stefan problem, *Num. Heat Transfer*, **1**, 351–364 (1978)

20 Comini, G., del Guidice, S., Lewis, R. W. and Zienkiewicz, O. C. Finite element solution of nonlinear conduction problems with special reference to phase change, *Int. J. Num. Meth. Eng.*, **8**, 613–624 (1974)
21 Morgan, K., Lewis, R. W. and Zienkiewicz, O. C. An improved algorithm for heat conduction problems with phase change, *Int. J. Num. Meth. Eng.*, **12**, 1191–1195 (1978)
22 O'Neill, K. Boundary integral equation solution of moving boundary phase change problems, *Int. J. Num. Meth. Eng.*, **19**, 1825–1850 (1983)
23 Zabaras, N. and Mukherjee, S. An analysis of solidification problem by the boundary element method, *Int. J. Num. Meth. Eng.*, **24**, 1879–1900 (1987)
24 Hseih, C. K., Choi, C. Y. and Kassab, A. J. Solution of Stefan problems by a boundary element method, *Boundary Element Technology VII*, C. A. Brebbia and M. S. Ingber, eds., Computational Mechanics Publications, Southampton, UK, 473–490 (1992)
25 Choi, C. Y. and Hsieh, C. K. Solution of Stefan problems imposed with cyclic temperature and flux boundary conditions, *Int. J. Heat Mass Transfer*, **35**, 1181–1195 (1992)
26 Hsieh, C. K. and Choi, C. Y. Solution of one- and two-phase melting and solidification problems imposed with constant or time-variant temperature and flux boundary conditions, *J. Heat Transfer*, **114**, 524–528 (1992)
27 Hsieh, C. K. and Choi, C. Y. A general analysis of phase change energy storage for solar energy applications, *J. Solar Energy Eng.*, **114**, 203–211 (1992)
28 Hseih, C. K., Akbari, M. and Li, H. Solution of inverse Stefan problems by a source-and-sink method, *Int. J. Num. Meth. Heat Fluid Flow*, **2**, 391–406 (1992)
29 Akbari, M. and Hsieh, C. K. Solution of ablation and combination of ablation and Stefan problems by a source-and-sink method, *Num. Heat Transfer*, **Part A**, 67–86 (1994)
30 Li, H. *Source-and-Sink Method of Solution of Two and Three Dimensional Stefan Problems*, PhD Dissertation, University of Florida (1993)
31 Gnielinski, V. New equations for heat and mass transfer in turbulent pipe and channel flow, *Int. Chem. Eng.*, **16**, 359–370 (1976)
32 Incropera, F. P. and Dewitt, D. P. *Fundamental of Heat and Mass Transfer* (*Third Edition*), John Wiley, New York (1990)
33 Barozzi, G. S. and Pagliarini, G. A method to solve conjugate heat transfer problems: The case of fully developed laminar flow in a pipe, *J. Heat Transfer*, **107**, 77–83 (1985)
34 Li, H., Hsieh, C. K. and Goswami, D. Y. Source and sink method of solution of two-dimensional phase change for energy storage, *J. Solar Energy Eng.*, **116**, 100–106 (1994)
35 Saitoh, T. and Hirose, K. High-performance phase-change thermal energy storage using spherical capsules, *Chem. Eng. Commun.*, **41**, 39–58 (1986)